ChemComm

COMMUNICATION

View Article Online
View Journal | View Issue

Cite this: *Chem. Commun.*, 2021, **57**, 10427

Received 23rd July 2021,
Accepted 13th September 2021

DOI: 10.1039/d1cc04001d

rsc.li/chemcomm

Low-dimensional magnetism in calcium nitridonickelate(II) Ca_2NiN_2†

Simon D. Kloß * and J. Paul Attfield *

Calcium nitridonickelate(II) Ca_2NiN_2 has been prepared through a high-temperature and high-pressure azide-mediated redox reaction, demonstrating that this method can stabilise nitrides of late transition metals in relatively high oxidation states. Ca_2NiN_2 crystallizes in the Na_2HgO_2 structure type and displays low-dimensional antiferromagnetic ordering of Ni^{2+} spins.

Multinary 3d transition metal nitrides have been extensively investigated with ambient and medium pressure (<1 GPa) synthesis methods for their diverse physical and electronic properties, their structural chemistry, and their close relation to the well-studied oxometallates.[1–7] However, access to nitrogen-rich transition metal nitrides is limited by the low energy of nitride formation[8–10] and especially for later transition metals such as Co, Ni and Cu, the obtainable nitrides are usually nitrogen-poor and metallic: while in molecular chemistry low-coordinate Ni^{II} imido complexes and a transient Ni^{IV} nitrido complex have been investigated,[11,12] currently reported solid-state nitridonickelates such as MNiN (M = Ca, Sr, Ba), $Ba_2Ni^{2/3+}{}_3N_2$, and $Li_3Sr_3Ni^{3/4+}{}_4N_4$,[13–17] feature low nitrogen to metal ratios and mean Ni oxidation states of 1+ or lower. LiNiN is the only well-characterized compound with Ni(II)[18] as a proposed Na_2HgO_2-type; the reported $Sr_2Ni^{II}N_2$ was later shown to be a cyano-nitridonickelate(0) *i.e.* $Sr_2[(NC)NiN]$.[19,20]

A higher nitrogen content could lead to opening of a band gap enabling semiconductivity, light-absorption for solar energy conversion applications, and emergence of localized-electron properties such as charge order and magnetism as found in oxo-metallates.[21–25] However, although recent high-throughput calculations have predicted many new nitride systems highlighting the great potential for materials discovery, employable synthesis routes for nitrogen rich compounds remain scarce.[9,26]

Applying high pressures in the gigapascal range is favorable for stabilizing nitrides against loss of dinitrogen but starting materials like transition metals or their binary nitrides often need to be nitrided *in situ*. This was demonstrated with N_2-loaded diamond anvil cell syntheses of binary materials such as metal diazenides and pernitrides like NiN_2 or PtN_2, polynitrides like FeN_4, and pentazolate salts like CsN_5.[27–30] Much less work has been done in multianvil large-volume presses but recently it was discovered that sodium azide can be used as a N_2 source, as demonstrated in the syntheses of rocksalt-type $Mg_{0.4}Fe_{0.6}N$ and the highly oxidized nitridoferrate(IV) Ca_4FeN_4.[31–33] Large-volume-presses offer the advantage over DACs that larger sample quantities for physical properties measurements can be prepared and multinary systems can more easily be studied.

Here we adapt the azide-route for the preparation of a new Na_2HgO_2-type nitridonickelate with Ni in the 2+ state, which is very unusual in this class of materials. Ca_2NiN_2 was obtained at 900 °C and 8 GPa following eqn (1) with a 10 mol% excess of Ca_3N_2 as a black moisture sensitive (lifetime in air several minutes) microcrystalline powder (Fig. S1, ESI†). The excess of Ca_3N_2 and NaN_3 is required to suppress the formation of byproduct CaNiN, which also forms when raising the temperature or lowering the pressure.[13]

$$6Ca_3N_2 + 9Ni + 4NaN_3 \rightarrow 9Ca_2NiN_2 + 4Na + 3N_2 \quad (1)$$

Ca_2NiN_2 was investigated with EDX spectroscopy showing a mean composition of $Ca_{2.0(2)}Ni_{0.9(1)}N_{2.0(2)}$ (normalized on Ca, 18 datapoints averaged, Table S1, ESI†). EDX also revealed that Na is finely dispersed throughout the sample (which precluded direct measurements of sample conductivity) and was identified through powder diffraction (Fig. 1a). There was no evidence of a Ca/Na mixed position through initial Rietveld refinement, consistent with Ca_4FeN_4, where the absence of Na incorporation was verified through Mössbauer and magnetization measurements.[32] The excess Ca_3N_2 might have formed an amorphous byproduct as the powder pattern showed a heightened background at low Q.

Centre for Science at Extreme Conditions, University of Edinburgh, Edinburgh EH9 3FD, UK. E-mail: v1skloss@ed.ac.uk, j.p.attfield@ed.ac.uk

† Electronic supplementary information (ESI) available. CCDC 2096979. For ESI and crystallographic data in CIF or other electronic format see DOI: 10.1039/d1cc04001d

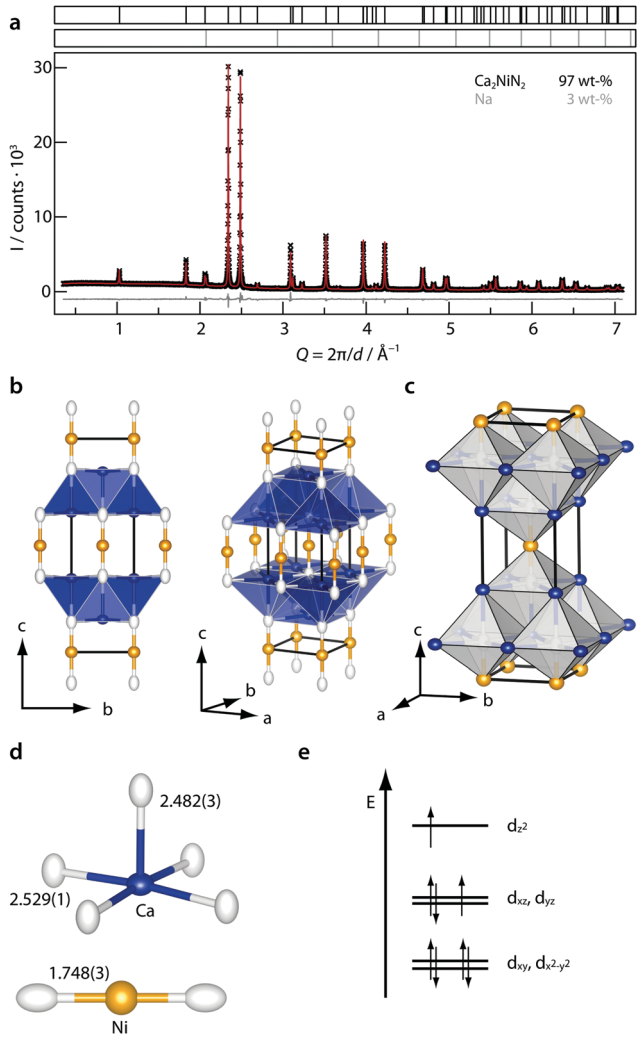

Fig. 1 (a) Rietveld refinement of Ca_2NiN_2 with datapoints as black crosses, Rietveld fit as red line, difference curve as grey line and tick marks of Ca_2NiN_2 and the Na byproduct shown above. The weight percent ratio of Ca_2NiN_2 and Na was refined to 97/3, which is in the range expected from stoichiometry, ideally 94/6. The diffuse background at low Q-values is probably due to amorphization of excess Ca_3N_2. (b–d) Structure of Ca_2NiN_2 with Ca as blue, Ni as orange and N as white ellipsoids at a 90% probability level. CaN_5 square pyramids are shown in blue and NCa_5Ni octahedra in grey. (e) Energy level diagram for d^8 Ni in linear coordination and simple σ-bonding adapted from literature.[11]

The crystal structure of Ca_2NiN_2 (space group $I4/mmm$, $Z = 2$, $a = 3.57206(2)$, $c = 12.19453(10)$ Å, $V = 155.719(5)$ Å^3) was determined from powder diffraction data by charge flipping in $P\bar{4}n2$ and subsequent refinement (Fig. 1a) in $I4/mmm$. Details and results of the refinement are in Tables S2 and S3 (ESI†).

Ca_2NiN_2 crystallizes in the Na_2HgO_2-structure type and features linear $[Ni^{II}N_2]^{4-}$ complex anions as well as layers of edge-sharing quadratic pyramids of CaN_5 (Fig. 1b) while the nitrogen atoms are coordinated by five Ca and one Ni atom forming layers of edge-sharing NCa_5Ni octahedra. In solid state chemistry, two-fold coordination of transition metals has for example been observed in Na_2HgO_2-type compounds such as M_2NiO_2 (M = K, Rb and Cs) and A_2ZnN_2 (A = Ca, Sr, Ba), and nitridometallates of Co, Ni and Cu with either linear chains, kinked chains, or $[MN_2]$-dumbbells such as AMN-type compounds, $(BaCa_4[MN_2]_2)$ (M = Co, Cu) and $Sr_{39}Co_{12}N_{31}$.[34–40] The interatomic distances in the CaN_5 square pyramid (Fig. 1c) are equal in the equatorial plane and both Ca–N distances (Fig. 1d) are in the range observed in similar compounds like CaNiN, Ca_2ZnN_2, Ca_2FeN_2, Ca_4FeN_4, $Ca_5Co_2N_4$, and Ca_3N_2 (d_{Ca-N} = 2.40–2.82 Å).[13,32,36,41–43] The Ni–N distance observed in Ca_2NiN_2 is smaller than in compounds containing infinite N–Ni–N chains like $CaNi^{I}N$ (d_{Ni-N} = 1.792(1) Å) and $BaNi^{I}N$ (d_{Ni-N} = 1.8281(1), 1.781(1) Å), which is probably owed to the higher oxidation state of Ni and the terminal Ni–N bonds.[13,17]

Bond valence sum (BVS) calculations were performed for Ca and Ni for a coordination sphere of 4 Å using bond valence parameters reported by O'Keeffe (Table S3, ESI†). The bond valence sum for Ni $V_{Ni,N}$ = 2.03 corroborates the presence of Ni^{II}, while the bond valence sum for Ca is slightly lower with V_{Ca-N} = 1.80.[44] This is probably owed to the covalent bonding in nitrides and metal–metal interactions and has also been observed in related compounds such as CaGaN (V_{Ga-N} = 0.9), Ca_4FeN_4 (V_{Ca-N} = 1.85, 1.65), and the isotypic Ca_2ZnN_2 (V_{Ca-N} = 1.82).[32,35,45,46]

Magnetic susceptibility measurements (Fig. 2) carried out at 30 kOe in the temperature range from 2.5 to 300 K showed a broad maximum at *ca.* 200 K and a decrease towards lower temperatures. The higher temperature region of the susceptibility is indicative of short-range low-dimensional antiferromagnetic spin interactions, which also has been observed in related nitridometallates such as Ca_3CrN_3 and $Ba_4Mn_3N_6$.[23,47] The derivative $d\chi/dT$ (Fig. S2, ESI†) shows a maximum at T_N = 74 K indicating the possible onset of long-range magnetic ordering. Neutron diffraction data will be needed to confirm this.

The susceptibility data were fit according to $\chi_{mol} = \chi_C + \chi_{BF}$ with a Bonner–Fisher-type function χ_{BF} and a Curie function χ_C to account for an impurity producing a Curie tail at low temperatures (see methods for details, ESI†).[48] The resulting fit (Fig. 2) follows the data well, with a deviation below ~75 K close to the maximum in $d\chi/dT$ at 74 K (Fig. S2, ESI†). The fitted

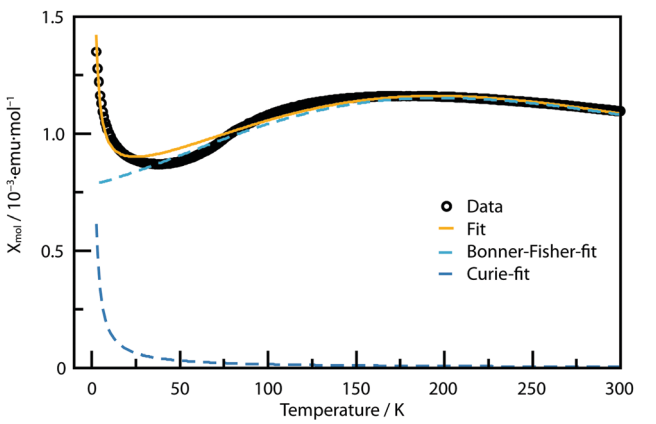

Fig. 2 Magnetic molar susceptibility of Ca_2NiN_2 measured in a field of 30 kOe with black circles as datapoints and combined Bonner–Fisher and Curie-tail fit as orange line.

paramagnetic moment of μ_{eff} = 2.19 μ_B is reduced from the ideal S = 1 spin-only value of 2.83 μ_B, most likely due to mixing with excited states through spin–orbit coupling. The fitted exchange coupling of J = −157 K confirms strong antiferromagnetic coupling within the *ab*-planes. Both the μ_{eff} and J values are consistent with localised Ni^{2+} moment behavior. The impurity phase has an effective moment of 0.11 μ_B, equivalent to 0.4% of a $S = \frac{1}{2}$ byproduct, which is below the detection limit of powder diffraction. The low-dimensional magnetic behavior reflects the arrangement of Ni-atoms in square nets with interatomic distances of d_{Ni-Ni} = 3.572(1) Å, which are separated by layers of CaN_5 square-pyramids. Field-dependent magnetization data at 300 and 2.5 K (Fig. S2, ESI†) shows a linear dependence in accordance with paramagnetic or antiferromagnetic behavior.

The high-temperature behavior of Ca_2NiN_2 was investigated with temperature-dependent powder X-ray diffraction (Fig. 3) and reveals Vegard-type behavior of the lattice parameters up to 600 °C with thermal expansion coefficients of $\alpha_a = 1.8(1) \times 10^{-5}$ K^{-1} and $\alpha_c = 7.1(6) \times 10^{-6}$ K^{-1}. The larger value of α_a reflects greater amplitudes of thermal vibration perpendicular to the NiN_2 dumbbells which are aligned in the *c*-direction. Above this temperature Ca_2NiN_2 starts to decompose through elimination of $\frac{1}{2}$ N_2 and 1 Ca per formula unit resulting in crystalline CaNiN.[13] Ca/Ca_3N_2 could not unambiguously be identified in the powder patterns and might also be amorphous. The decomposition was monitored through phase fractions, which show gradual decomposition over a wider temperature range, which might be owed to the relatively fast data collection of 30 min per step. At 960 °C the capillary presumably broke as CaNiN, which was reported to be stable up to 1100 °C, decomposed into CaO and metallic Ni.[6]

In conclusion, the preparation of Ca_2NiN_2 with Ni in oxidation state +II, which is very unusual for nitridometallates, is demonstrated through the azide-mediated nitridation of metallic Ni under high-pressure conditions. Ca_2NiN_2 crystallizes in the Na_2HgO_2 structure type with linear coordination of Ni. While in molecular chemistry low metal coordination environments are stabilized through sterically demanding ligands, the stabilization here is probably due to covalent Ni–N multiple bonding and consequent short Ni–N bond distances and the electron inductive effect of the surrounding Ca^{2+} matrix.[49] The observation of a susceptibility maximum consistent with low-dimensional antiferromagnetic ordering of Ni^{2+} spins in Ca_2NiN_2, whereas metallic CaNiN has a temperature-independent Pauli susceptibility, suggests that Ca_2NiN_2 is non-metallic but further measurements will be required to confirm this. Temperature-dependent powder X-ray diffraction shows that Ca_2NiN_2 is stable up to 600 °C before decomposing to CaNiN, which when compared to the synthesis temperature of 900 °C indicates the stabilizing influence of the high-pressure conditions. Stability estimates are particularly important for efficient planning of syntheses of compounds of noble metals like Ni and Cu, and our results highlight that nitrogen-rich compounds require very stringent temperature control which necessitates synthesis under a high nitrogen chemical potential. Discovery of Ca_2NiN_2 indicates that a new class of late transition metal nitrides can be synthesised, and like oxo-nickelates and -cuprates, they may have interesting correlated electron properties in proximity to a metal–insulator boundary, as illustrated by the recent discovery of superconductivity in infinite-layer nickelates $LnNiO_2$.[50]

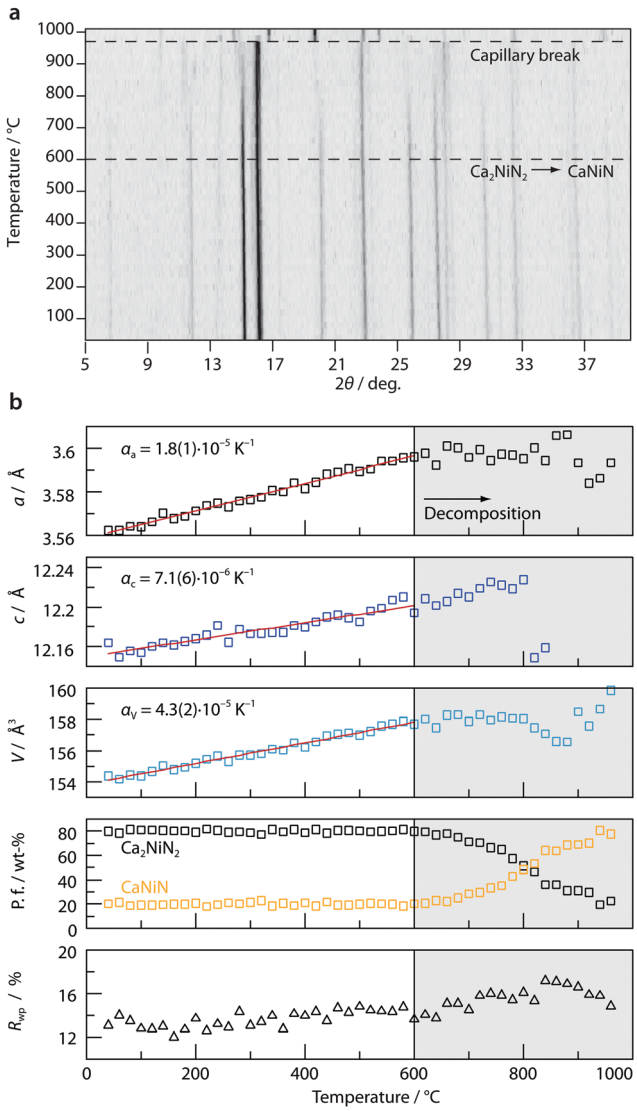

Fig. 3 (a) Temperature-dependent PXRD of a Ca_2NiN_2 sample containing a 20 wt% impurity of CaNiN. Dashed lines indicate decomposition onset and capillary break. (b) Results of the Rietveld analysis up to 960 °C showing evolution of lattice parameters *a*, *c*, and volume *V* with temperature as well as the decomposition of Ca_2NiN_2 into CaNiN as a function of phase fraction (p. f.). Linear regressions (red lines) were used to extract thermal expansion parameters of Ca_2NiN_2. The fit quality is monitored through R_{wp}, which increases with temperature owed to decreasing data quality. Estimated standard deviations (ESD) of individual datapoints are too small to be displayed.

Conflicts of interest

There are no conflicts to declare.

Notes and references

1 R. Niewa and F. J. DiSalvo, *Chem. Mater.*, 1998, **10**, 2733.
2 H. Yamane and F. J. DiSalvo, *Prog. Solid State Chem.*, 2018, **51**, 27.
3 N. Tapia-Ruiz, M. Segalés and D. H. Gregory, *Coord. Chem. Rev.*, 2013, **257**, 1978.
4 J. M. Cameron, R. W. Hughes, Y. Zhao and D. H. Gregory, *Chem. Soc. Rev.*, 2011, **40**, 4099.
5 R. Niewa and H. Jacobs, *Chem. Rev.*, 1996, **96**, 2053.
6 F. J. DiSalvo and S. J. Clarke, *Curr. Opin. Solid State Mater. Sci.*, 1996, **2**, 241.
7 F. J. DiSalvo, *Science*, 1990, **247**, 649.
8 D. R. Glasson and S. A. A. Jayaweera, *J. Appl. Chem.*, 1968, **18**, 65.
9 W. Sun, A. Holder, B. Orvañanos, E. Arca, A. Zakutayev, S. Lany and G. Ceder, *Chem. Mater.*, 2017, **29**, 6936.
10 A. Salamat, A. L. Hector, P. Kroll and P. F. McMillan, *Coord. Chem. Rev.*, 2013, **257**, 2063.
11 P. P. Power, *Chem. Rev.*, 2012, **112**, 3482–3507.
12 V. Vreeken, M. A. Siegler, B. de Bruin, J. N. H. Reek, M. Lutz and J. I. van der Vlugt, *Angew. Chem., Int. Ed.*, 2015, **54**, 7055 (*Angew. Chem.*, 2015, **127**, 7161–7165).
13 M. Y. Chern and F. J. DiSalvo, *J. Solid State Chem.*, 1990, **88**, 459.
14 T. Yamamoto, S. Kikkawa and F. Kanamaru, *J. Solid State Chem.*, 1995, **115**, 353.
15 A. Gudat, R. Kniep and A. Rabenau, *Z. Anorg. Allg. Chem.*, 1991, **597**, 61.
16 A. Mehta, P. Höhn, W. Schnelle, V. Petzold, H. Rosner, U. Burkhardt and R. Kniep, *Chem. – Eur. J.*, 2006, **12**, 1667.
17 A. Gudat, S. Haag, R. Kniep and A. Rabenau, *J. Less-Common Met.*, 1990, **159**, L29.
18 C. H. Hu, Y. Yang and Z. Z. Zhu, *Solid State Commun.*, 2010, **150**, 669.
19 G. R. Kowach, N. E. Brese, U. M. Bolle, C. J. Warren and F. J. DiSalvo, *J. Solid State Chem.*, 2000, **154**, 542.
20 P. Höhn, M. Armbrüster, G. Auffermann, U. Burkhardt, F. Haarmann, A. Mehta and R. Kniep, *Z. Anorg. Allg. Chem.*, 2006, **632**, 2129.
21 P. Chanhom, K. E. Fritz, L. A. Burton, J. Kloppenburg, Y. Filinchuk, A. Senyshyn, M. Wang, Z. Feng, N. Insin, J. Suntivich and G. Hautier, *J. Am. Chem. Soc.*, 2019, **141**, 10595.
22 M. Yang, A. Zakutayev, J. Vidal, X. Zhang, D. S. Ginley and F. J. DiSalvo, *Energy Environ. Sci.*, 2013, **6**, 2994.
23 D. A. Vennos, M. E. Badding and F. J. DiSalvo, *Inorg. Chem.*, 1990, **29**, 4059.
24 R. Marchand and V. Lemarchand, *J. Less-Common Met.*, 1981, **80**, 157.
25 A. Zakutayev, *J. Mater. Chem. A*, 2016, **4**, 6742.
26 W. Sun, C. J. Bartel, E. Arca, S. R. Bauers, B. Matthews, B. Orvañanos, B.-R. Chen, M. F. Toney, L. T. Schelhas, W. Tumas, J. Tate, A. Zakutayev, S. Lany, A. M. Holder and G. Ceder, *Nat. Mater.*, 2019, **18**, 732.
27 K. Niwa, R. Fukui, T. Terabe, T. Kawada, D. Kato, T. Sasaki, K. Soda and M. Hasegawa, *Eur. J. Inorg. Chem.*, 2019, 3753–3757.
28 J. C. Crowhurst, *Science*, 2006, **311**, 1275.
29 M. Bykov, E. Bykova, G. Aprilis, K. Glazyrin, E. Koemets, I. Chuvashova, I. Kupenko, C. McCammon, M. Mezouar, V. Prakapenka, H.-P. Liermann, F. Tasnádi, A. V. Ponomareva, I. A. Abrikosov, N. Dubrovinskaia and L. Dubrovinsky, *Nat. Commun.*, 2018, **9**, 2756.
30 D. Laniel, G. Weck, G. Gaiffe, G. Garbarino and P. Loubeyre, *J. Phys. Chem. Lett.*, 2018, **9**, 1600.
31 G. Serghiou, G. Ji, N. Odling, H. J. Reichmann, J.-P. Morniroli, R. Boehler, D. J. Frost, J. P. Wright and B. Wunder, *Angew. Chem., Int. Ed.*, 2015, **54**, 15109 (*Angew. Chem.*, 2015, **127**, 15324).
32 S. D. Kloß, A. Haffner, P. Manuel, M. Goto, Y. Shimakawa and J. P. Attfield, *Nat. Commun.*, 2021, **12**, 571.
33 M. Bykov, K. R. Tasca, I. G. Batyrev, D. Smith, K. Glazyrin, S. Chariton, M. Mahmood and A. F. Goncharov, *Inorg. Chem.*, 2020, **59**, 14819.
34 T. Yamamoto, S. Kikkawa and F. Kanamaru, *Solid State Ionics*, 1993, **63–65**, 148.
35 H. Rieck and R. Hoppe, *Z. Anorg. Allg. Chem.*, 1973, **400**, 311.
36 M. Y. Chern and F. J. DiSalvo, *J. Solid State Chem.*, 1990, **533**, 528.
37 H. Yamane and F. J. DiSalvo, *J. Solid State Chem.*, 1995, **119**, 375.
38 J. K. Bendyna, P. Höhn, Y. Prots and R. Kniep, *Z. Kristallogr. - New Cryst. Struct.*, 2007, **222**, 484.
39 G. R. Kowach, H. Y. Lin and F. J. Disalvo, *J. Solid State Chem.*, 1998, **9**, 1–9.
40 R. Niewa and F. J. DiSalvo, *J. Alloys Compd.*, 1998, **279**, 153–160.
41 P. Höhn and R. Kniep, *Z. Naturforsch.*, 1992, **47b**, 477–481.
42 J. K. Bendyna, P. Höhn and R. Kniep, *Z. Kristallogr. - New Cryst. Struct.*, 2007, **222**, 165.
43 Y. Laurent, J. Lang and M. T. Le Bihan, *Acta Crystallogr., Sect. B: Struct. Crystallogr. Cryst. Chem.*, 1968, **24**, 494.
44 N. E. Brese and M. O'Keeffe, *Acta Crystallogr., Sect. B: Struct. Sci.*, 1991, **47**, 192.
45 N. E. Brese and M. O'Keeffe, *Crystal chemistry of inorganic nitrides in Complexes, Clusters and Crystal Chemistry*, Springer-Verlag, Berlin/Heidelberg, 2006, p. 307.
46 D. H. Gregory, *J. Chem. Soc., Dalton Trans.*, 1999, 259.
47 A. Ovchinnikov, M. Bobnar, Y. Prots, W. Schnelle, P. Höhn and Y. Grin, *Crystals*, 2018, **8**, 235.
48 M. E. Fisher, *Am. J. Phys.*, 1964, **32**, 343.
49 J. Etourneau, J. Portier and F. Ménil, *J. Alloys Compd.*, 1992, **188**, 1.
50 D. Li, K. Lee, B. Y. Wang, M. Osada, S. Crossley, H. R. Lee, Y. Cui, Y. Hikita and H. Y. Hwang, *Nature*, 2019, **572**, 624.

